CrossMark

Electrical characterizations of Au/ZnO/n-GaAs Schottky diodes under distinct illumination intensities

S. O. Tan[1] · H. Uslu Tecimer[2] · O. Çiçek[3] · H. Tecimer[4] · İ. Orak[5] ·
Ş. Altındal[6]

Abstract The Au/ZnO/n-GaAs Schottky barrier diode was fabricated and examined regarding to its current–voltage characteristics under distinct illumination intensities at room temperature. The reverse biased current increases with increasing illumination level while forward biased current is almost unchanged with illumination which states that the fabricated diodes exhibit photosensitive character or photodiode behavior. Hence, the shunt resistance is decreased with illumination while the series resistance is almost remained constant. The increment in the ideality factor after illumination can be ascribed to the assumption of inhomogeneities at M/S interface. Considering the ideality factor and the voltage dependent effective barrier height, the energy distribution profiles of surface states (N_{ss}) were formed by the forward bias current–voltage data and increased with increasing illumination level. The Nss values acquired by considering series resistance are lower than those acquired by ignoring series resistance. Consequently, surface states can serve as recombination centers and have great importance especially in reverse bias current–voltage characteristics.

✉ S. O. Tan
serhatorkuntan@karabuk.edu.tr

H. Uslu Tecimer
habibeuslu@karabuk.edu.tr

O. Çiçek
ocicek@kastamonu.edu.tr

H. Tecimer
huseyintecimer@karabuk.edu.tr

İ. Orak
iorak@bingol.edu.tr

Ş. Altındal
altundal@gazi.edu.tr

[1] Karabuk Vocational School, Karabuk University, Karabük, Turkey

[2] Department of Electrical and Electronic Engineering, Faculty of Engineering, Karabük University, Karabük, Turkey

[3] Arac Vocational School, Kastamonu University, Kastamonu, Turkey

[4] Department of Mechatronics Engineering, Faculty of Technology, Karabük University, Karabük, Turkey

[5] Vocational School of Health Services, Bingöl University, Bingöl, Turkey

[6] Department of Physics, Faculty of Science, Gazi University, Ankara, Turkey

1 Introduction

Having attracted great interest for their importance in electronic and optoelectronic devices, solid electronic devices can be understood better by seriously considering metal–semiconductor (MS) structures [1–6]. Therefore, many attempts have been made to improve the MS structure quality of the Schottky barrier diodes (SBDs) and obtain continuous control of the barrier height (BH) by using a high dielectric value of an insulator or organic interfacial layer instead of classic/conventional SiO_2. Thus, the insertion of a thin interfacial insulator layer to the M/S interface transforms the structure to metal–insulator-semiconductor which can be abbreviated as MIS type SBDs [4–7]. Gallium Arsenide (GaAs) was mentioned at numerous scientific studies on MS and MIS type SBDs or structures [8–11]. As a multipurpose semiconductor, GaAs has also been used in many applications such as field effect transistor (FET), solar cells (SCs), light emitting diodes (LEDs), microwave devices, integrated circuit elements, etc. Direct forbidden bandgap, high electron mobility,

lower power dissipation, a high break-down voltage and mechanical stability are very significant properties that lead to widespread usage of the GaAs at high-speed and low-power devices [12–15]. Now, there is extensive information about metal contacts on gallium arsenide due to the evolvements on GaAs electronic devices [15]. The applied bias voltage, series resistance (R_s), surface preparation, interface/surface states density (N_{ss}), doping concentration of acceptor (N_A) or donor atoms (N_D) at M/S interface, frequency and temperature have significant effects on BH formation and also transport mechanism at the GaAs based devices [15–21]. In addition, the quality of this interface layer and its thickness between deposited material and the surface of the semiconductor strongly affects the performance and also the reliability of the MIS/MPS SBDs [22–26].

Several materials were used as an interface layer. Among them zinc oxide (ZnO) is frequently utilized material, which appears to be an effective inorganic interfacial layer at GaAs based SBDs. High transparency, piezoelectricity, ferromagnetism at room-temperature are some superior properties of the wide band gap ZnO which make it a commonly used material in many applications such as polariton lasers, UV photodetectors, piezotronics, etc. [27–29]. As also used in this study, Au/ZnO has been used several times by the research community for examining the current-transport mechanisms of SBDs via the current–voltage (I–V) measurements [28–30]. The interfacial layer, ZnO, substantially changes the characteristics of the SBDs by considering the ideal behavior. Furthermore, there are various factors as barrier height (Φ_{Bo}) from metal to semiconductor, thickness of the insulator (d_{ox}) and also N_{ss} and R_s parameters which can bring the structure to the non-ideal case [31].

The semi logarithmic scaled I–V characteristics at low forward biases are generally linear. On the other hand, in case of an adequately large forward biases, R_s, N_{ss} and interfacial layer parameters give rise to deviation from these linear characteristics [31–35]. Although the R_s effect can only be sighted in the curvature downward region, the N_{ss} parameter, together with a change of the Schottky BH, is effectual in the linear and also non-linear regions of these characteristics [36, 37]. Electrical parameters of SBDs are exceptionally relevant with the intensity of illumination level, so the analysis of SBDs should be made not only in dark but also in different illumination levels to inform the structural parameters of devices [38, 39]. Therefore, the investigation of the electrical and photo-response qualifications of the fabricated Au/ZnO/n-GaAs SBDs in the 0–200 W illumination range is the main purpose of this study. Furthermore, the electrical characteristics of the SBDs have been studied under ordinary room temperature conditions by using the I–V measurements in both forward and reverse biases. The voltage dependence resistance, the series and also the shunt resistance (R_{sh}) of the SBDs were extracted from Ohm's law. The methods of Cheung and Norde were used to achieve and compare the series resistance values. Moreover, the energy density distribution profile of N_{ss} were acquired from the I–V data in forward biases by considering R_s, n and voltage dependent BH. Experimental results indicated that an increment in the n values and a decrement in the Φ_{Bo} values were observed with an increasing in illumination level.

2 Experimental procedure

GaAs (100) n-type wafer was used to prepare Au/ZnO/n-GaAs/Au SBDs as substrate with thickness and resistivity values of 300 μm and 1–10 Ω cm respectively. The wafer n-type GaAs was cut into pieces of 1.0 cm length by 1.0 cm breadth. The wafer was chemically cleaned by using acetone, isopropyl alcohol ultrasonic cleaner for five min and then quenched in deionized water. The high pure (99.999 %) Au (150 nm) metal was evaporated on the back side of the n-GaAs in high-vacuum metal evaporation system at about 10^{-6} Torr. After that, annealing process for wafers took 3 min times at 500 °C in N_2 atmosphere to get low resistivity ohmic back contact. Then, chemical compound of HF + 10H_2O was used for the disposal of the native oxide on the front surface of the substrate. The contact was dried with N_2 after rinse processing which took 30 s in de-ionized water. The ZnO (50 nm) film was grown on n-GaAs substrates by RF-magnetron sputtering technique and controlled thickness with thickness monitor. Finally the upper rectifier/Schottky contacts with 1 mm radius (=7.85 × 10^{-3}cm^2 area) as constituted by thermal evaporating Au (150 nm). The processes of evaporation and coating were performed in the unit of vacuum coating at 4.10^{-6} Torr. Thus the fabrication processes of MIS type SBDs were completed. In order to fulfil the I–V data measurements, SBDs were put on the Cu-holder and then electrical contacts were connected to the upper electrode by thin Cu wires and Si dag. The current–voltage data of the SBDs have been performed using a Keithley 4200 current/voltage source at ordinary room temperature and they controlled by a software programme used with IEEE-488 AC/DC converter. In addition, to prevent any noise or environmental conditions, the measurements were carried out in Janis VPF-4785 cryostat at about 10^{-3} Torr.

Newport-Oriel (Model: 69931) 250 W solar simulator used as a light source for illuminating the sample and International Light Technologies radiometer (Model ILT1700) used to measure the illumination intensity. Figure 1 presents the schematic diagram of the Au/ZnO/n-GaAs SBDs under incident light.
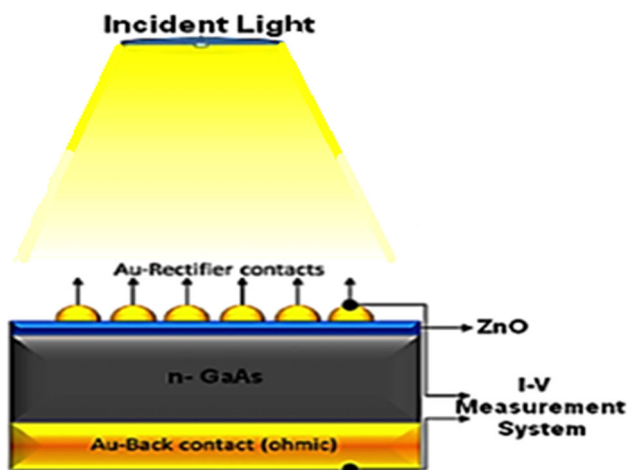
Fig. 1 The connection of the measurement system to Au/ZnO/*n*-GaAs SBDs under a light source

3 Results and discussion

The Au/ZnO/*n*-GaAs SBDs current versus voltage characteristics examined at forward and also reverse biased regions are indicated in Fig. 2 in a semi-logarithmic scale. The effect of increasing illumination levels and also darkness are presented in Fig. 2. The increment behavior monitored in reverse biased current of the SBDs with increasing illumination level can be interpreted as a
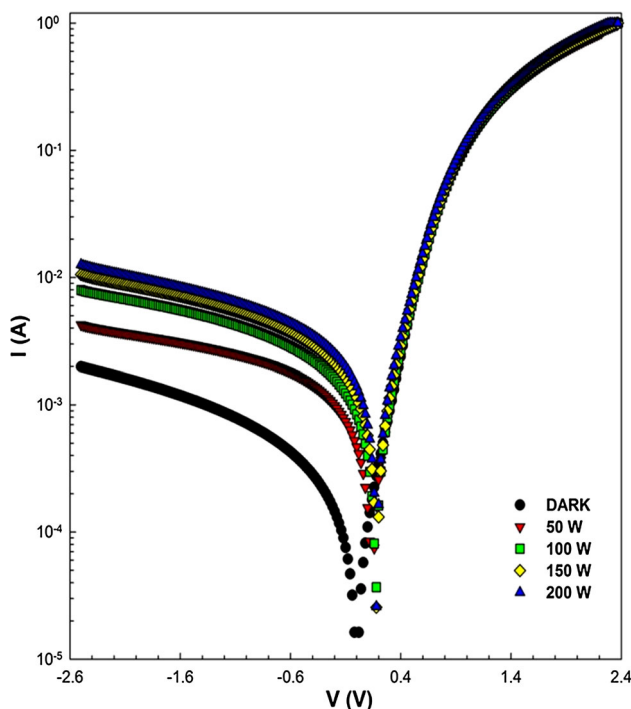

Fig. 2 The *I–V* characteristics of Au/ZnO/*n*-GaAs SBDs under specific illumination levels

photodiode behavior. In other words, the fabricated SBDs exhibit a photodiode behavior. The structure behaves like a SBDs and the forward biases current–voltage characteristics for SBDs with a series resistance (R_s) obey the thermionic emission model as below [1, 5, 8].

$$I = I_o \exp\left(\frac{q(V - IR_s)}{nkT}\right)\left[1 - \exp\left(\frac{-q(V - IR_s)}{kT}\right)\right] \quad (1)$$

Here, q is the electron charges, T is the temperature in Kelvin, V is the voltage applied on the Schottky junction, and the term of IR_s is the voltage drop on the R_s and k is the Boltzmann constant. The voltage drop on the diode can be expressed by the difference between the total voltage drop and the potential on the series resistance as $V - IR_s$ while $V > 3kT/q$. Here, the saturation current Io can be derived from an intercept of a straight line of $ln(I)$ at zero bias as shown below in Eq. (2).

$$I_o = AA^*T^2 \exp\left(-\frac{q\Phi_{Bo}}{kT}\right) \quad (2)$$

The diode area is denoted by A and the Richardson constant is denoted by A^* which equals to 8.16 A/cm² K² for *n*-GaAs. The zero bias BH can also be extracted from Eq. (2).

$$\Phi_{Bo} = \frac{kT}{q}\ln\left(\frac{AA^*T^2}{I_o}\right) \quad (3)$$

The n value exceeded unity due to the existence of the R_s. The forward biases linear region slope of the $ln\ I$–V characteristic conduced to determined n from the equation below.

$$n = \frac{q}{kT}\frac{d(V - IR_s)}{d(\ln(I))} \quad (4)$$

The experimentally obtained values of I_o, n and Φ_{Bo} are given in Table 1. Both Table 1 and Fig. 3 verified that, there is an increase in ideality factor and a decrease in the zero-bias barrier height with an increment in the illumination levels.

The increment illumination level led to a decrease in the values of Φ_{Bo} and an increase in the values of n as represented in Table 1 ($\Phi_{Bo} = 0.410$ eV, n = 5.880 in dark and $\Phi_{Bo} = 0.395$ eV and $n = 6.721$ under 200 W). The increase of n after illumination can be explained by assuming inhomogeneities at M/S interface. In addition, the higher n values even in dark can be attributed to the presence of BH inhomogeneities and N_{ss} at M/S interface, R_s, interfacial ZnO layer and generation-recombination within the space charge region.

The voltage applied on the Schottky junction is shared out amongst interfacial and depletion layers and also the R_s of the diode structure. Since this shared voltage magnitude based on the thickness of the insulator layer, the shunt

Table 1 Illumination dependent electrical parameters values of Au/ZnO/n-GaAs SBDs

Power (W)	I_o (A)	n	Φ_{Bo} (eV)	Norde		Cheung		Ohm's law	
						dV/dln(I)	H (I)		
				R_s (Ω)	Φ_B (eV)	R_s (Ω)	R_s (Ω)	R_{sh} (Ω)	R_s (Ω)
0	4.03×10^{-4}	5.880	0.410	0.783	0.488	1.159	1.100	1254	2.379
50	4.58×10^{-4}	6.214	0.407	0.672	0.486	1.069	1.178	588	2.426
100	4.75×10^{-4}	6.214	0.406	0.588	0.485	1.066	1.178	407	2.392
150	5.72×10^{-4}	6.408	0.401	0.568	0.478	1.018	1.122	314	2.374
200	7.48×10^{-4}	6.721	0.395	0.479	0.471	0.989	1.033	267	2.360
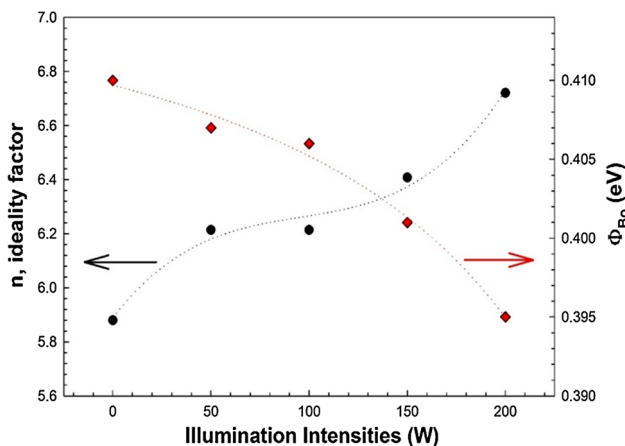
Fig. 3 The plots of Φ_{Bo} and n variation with illumination

Fig. 4 The voltage dependent resistance of the Au/ZnO/n-GaAs SBDs under distinct illumination levels

resistance (R_{sh}) and R_s are significant parameters that determine the reliability and the performance of SBDs. The increasing illumination level decreases the value of R_s on the occasion of the stimulation of the valance band charges to the conductance band. The effect of R_s can be seen as a downward curvature after 1 V level at high forward bias region from semi-logarithmic I–V plots in Fig. 2.

The voltage dependence resistance, the series and also the shunt resistance of the SBDs were derived from Ohm's law ($R_i = dV_i/dI_i$) and are also displayed in Table 1. The R_{sh} and R_s values were determined from the applied bias voltage (V) versus R_i plot in Fig. 4. Both resistance values decrease with the increment of the illumination levels and only the R_s values decrease with the increment of applied bias voltage as seen from Fig. 4.

The downward curvature effect of R_s mentioned above also reduces the forward biases $ln(I–V)$ curves linearity. N_{ss} and the insulator layer are also the reasons of this deviation from the linearity when a sufficiently high voltage is applied. Because, surface states serve as traps or recombination centers in the semiconductor, contingent on the capture cross-sections of the electron and holes.

When the forward and reverse bias lnI vs V plot has not enough large linear regions at intermediate bias region and considerably deviates from the linearity at enough high

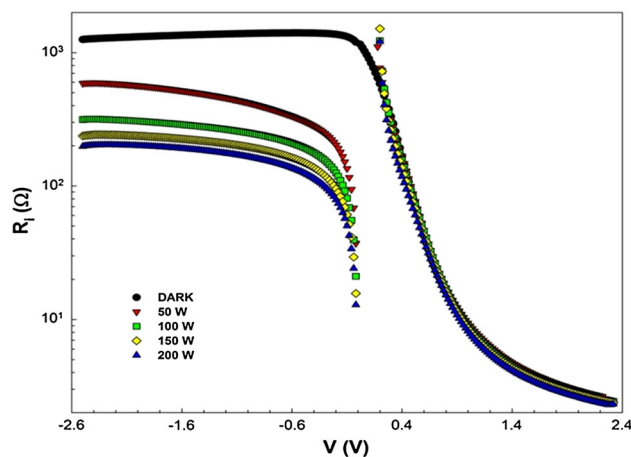bias voltages, then, the detection of the barrier height and also ideality factor loses some accuracy and becomes unreliable. Consequently, Cheung's method provided to achieve the R_s values under various illumination levels in the non-linear region of the forward biases I–V characteristics [40].

The value of R_s was determined and compared by Cheung and Cheung method by using following equations [40].

$$\frac{dV}{d(\ln I)} = n\frac{kT}{q} + IR_s. \tag{5}$$

$$H(I) = V - n\frac{kT}{q}\ln\left(\frac{I}{AA^*T^2}\right) = n\Phi_{Bo} + IR_s \tag{6}$$

Figure 5 shows the plots of $H(I)$ and $dV/dln(I)$ vs I that are examined in darkness and under distinct illumination intensities of the Au/ZnO/n-GaAs SBDs at ordinary room temperature conditions. R_s values have been achieved from the slope of the $dV/dln(I)$ vs I plots for each level of illumination as they can also be achieved from the Eq. (5). An alternative determination of the R_s provides to compare the consistency of the R_s values which can be obtained by the slope of $H(I)$ versus I plot. The R_s values derived from two equations above are in compliance and
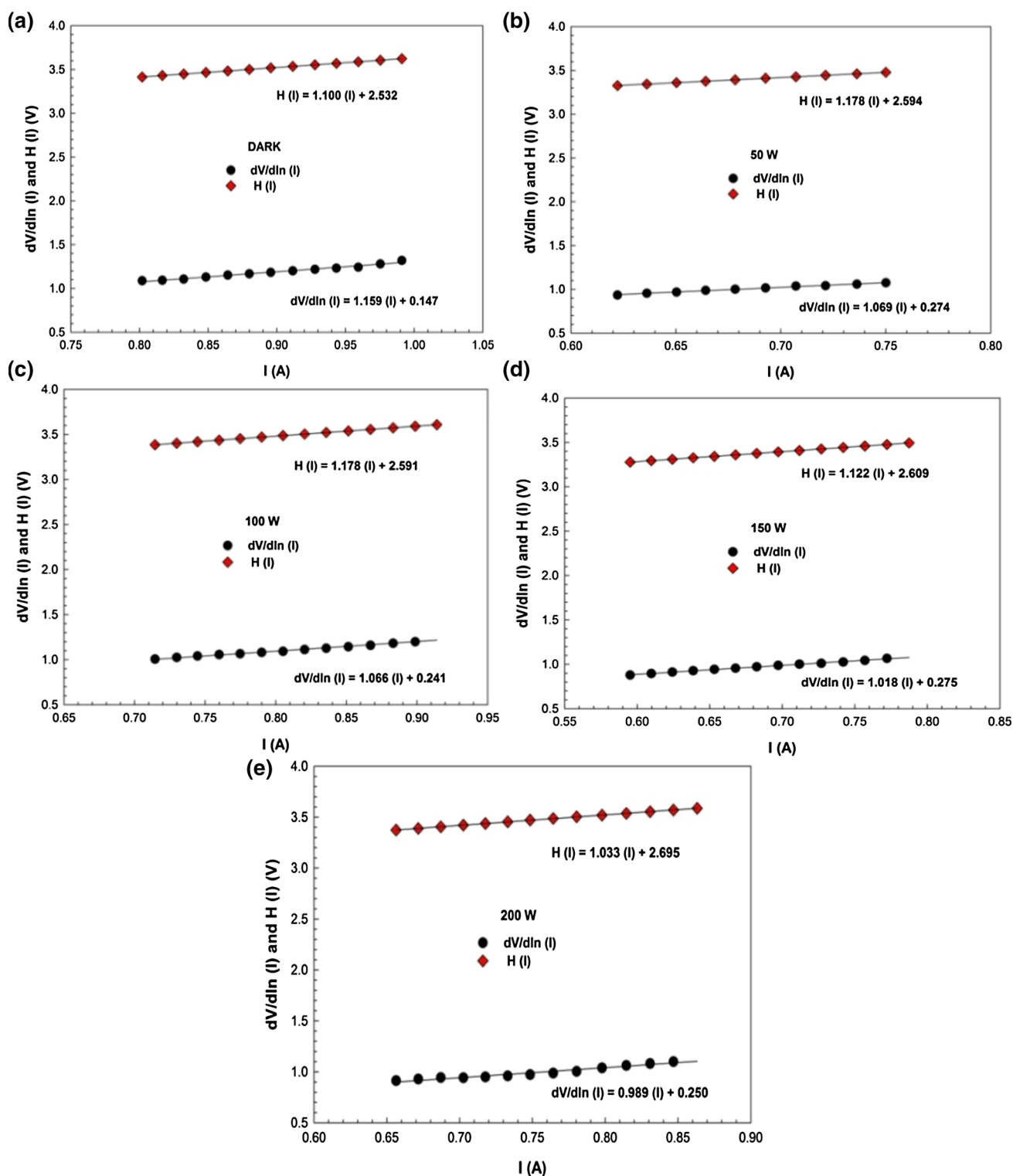
(a) H (I) = 1.100 (I) + 2.532

DARK

● dV/dln (I)
◆ H (I)

dV/dln (I) = 1.159 (I) + 0.147

(b) H (I) = 1.178 (I) + 2.594

50 W

● dV/dln (I)
◆ H (I)

dV/dln (I) = 1.069 (I) + 0.274

(c) H (I) = 1.178 (I) + 2.591

100 W

● dV/dln (I)
◆ H (I)

dV/dln (I) = 1.066 (I) + 0.241

(d) H (I) = 1.122 (I) + 2.609

150 W

● dV/dln (I)
◆ H (I)

dV/dln (I) = 1.018 (I) + 0.275

(e) H (I) = 1.033 (I) + 2.695

200 W

● dV/dln (I)
◆ H (I)

dV/dln (I) = 0.989 (I) + 0.250

Fig. 5 The plots of $dV/dlnI$ versus I and $H(I)$ versus I under distinct illumination levels

decreasing by increasing illumination intensities as clearly seen in Table 1. There are several studies in the literature showing similar variations of R_s depending on the increasing illumination level [41–44]. Concerning to the illumination effect, the results display consistency with the decrement of the density of carriers in the depletion region through recombination centers and entry of traps [45].

The energy density distribution profile of N_{ss} can easily be determined by considering the R_s values, the effective barrier height (Φ_e) and the voltage dependent ideality factor (n (V)). The following equations are given for calculation of $n(V)$ and Φ_e, respectively [34].

$$\text{n (V)} = 1 + \delta/\varepsilon_i[\varepsilon_s/W_D + qN_{SS} \text{ (V)}] \qquad (7)$$

$$\Phi_e = \Phi_{Bo} + \beta (V - IR_s) \qquad (8)$$

The effective barrier height voltage coefficient is termed as β parameter which is defined by the Eq. (9).

$$\beta = \partial\Phi_e/\partial V = 1 - 1/(n(V)) \qquad (9)$$

β parameter also includes both N_{ss} effects with the semiconductor in equilibrium. Card and Rhoderick suggested the simplified form of the interface states density equation which was stated as below [34].

$$N_{ss}(V) = \frac{1}{q}\left[\frac{\varepsilon_i}{\delta}(n(V) - 1) - \frac{\varepsilon_s}{W_D}\right] \qquad (10)$$

Here, W_D and δ can be expressed as the depletion layer width and the interfacial inorganic insulator layer thickness respectively. The permittivity parameters of the semiconductor and the interfacial insulator layer are denoted by ε_i and ε_s. Additionally, the energy of interface states (E_{ss}) with regard to the lowermost level of the conduction band (E_c) at the n-type semiconductors surface can be achieved from the below equation.
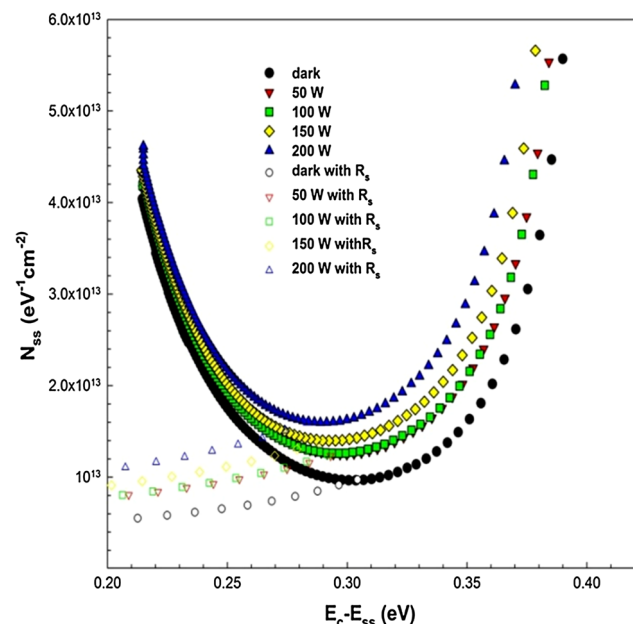
$$E_c - E_{ss} = q(\Phi_e - V) \qquad (11)$$

Considering the effective barrier height at forward biases in darkness and under specified illumination intensities, N_{ss} versus ($E_c - E_{ss}$) were given in Fig. 6 by substituting $n(V)$, δ and W_D values in Eq. (10).

The exponentially increasing behavior of the N_{ss} through the conduction band is obviously seen from the figure above. Furthermore, the N_{ss} values increased with illumination between (E_c-0.21) and (E_c-0.39) eV interval. When R_s was included, N_{ss} value decreased nearly five times as it is shown in Fig. 6. We also benefited from the Norde method to examine the R_s and the BH values of the Au/ZnO/n-GaAs SBDs. The equation below indicates the modified function of Norde's method.

$$F(V) = \frac{V}{\gamma} - \frac{kT}{q}\ln\left(\frac{I(V)}{AA^*T^2}\right) \qquad (12)$$

Here; the I–V curve was used to determine the $I(V)$ current and γ can be stated as the first integer greater than the ideality factor. Identifying $F(V_o)$ as the minimum point of $F(V)$ vs V plot (Fig. 7) and the quantities of V_o and I_o corresponding to the minimum this point.

$$\Phi_B = F(V_o) + \frac{V_o}{\gamma} - \frac{kT}{q} \qquad (13)$$

$F(V)$ vs V plots of the Au/ZnO/n-GaAs SBDs under specified illumination conditions are shown in Fig. 7. Norde's functions calculated the value of R_s as below.

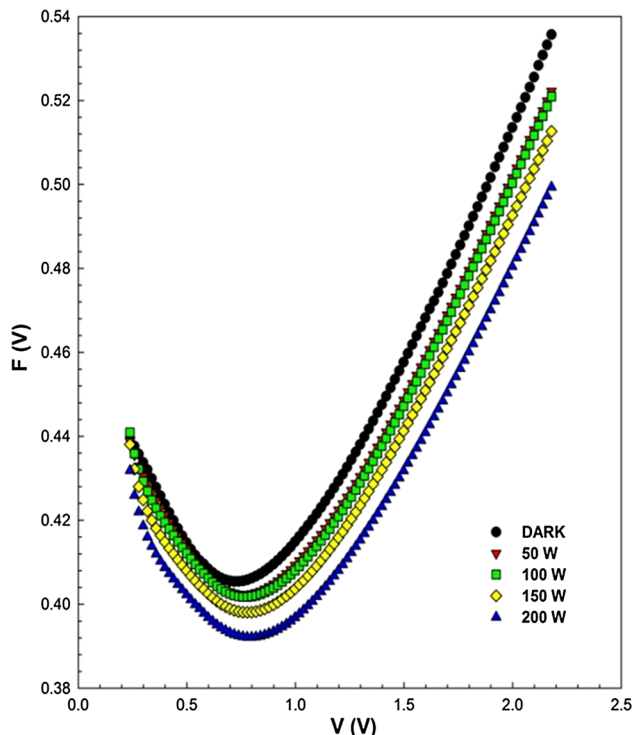Fig. 6 R_s effect under specified illumination levels on the energy distribution profile of N_{ss}

Fig. 7 The F(V) versus V plots of theAu/ZnO/n-GaAs SBDs under distinct illumination levels

$$R_s = \frac{kT(\gamma - n)}{qI_o} \qquad (14)$$

Analyzing the values given in Table 1, the R_s and BH values are decreasing by the increasing illumination intensities. The decrement of the R_s values with increasing illumination intensity was commonly observed in both Cheung and Norde methods.

4 Conclusions

The Au/ZnO/n-GaAs SBDs have been fabricated and their I–V characteristics at two biases were examined in darkness and also distinct illumination levels. The electrical parameters of the diode were found as a strong function of illumination and applied bias voltage. Under illumination, electrons in the valance band and traps absorb adequate energy and so they are easily jumped to the conductance band. Also, the reverse current at a given voltage always higher than that of the current in darkness and it increases with increasing illumination level. Because under reverse bias, both interior electric field and external electric field are the same direction and so the created electron–hole pairs recombination becomes very hard under this high electric field. The obtained n and Φ_{Bo} values imply that the increment at n values is inversely proportional with Φ_{Bo} values for increasing illumination intensity conditions. Ohm's law was used to get the voltage dependent profiles of resistivity (R_i) values from the I–V curves. Thus, the values of R_s and R_{sh} of the SBDs were revealed from the $R_i - V_i$ plots as 2.379Ω and 1254 Ω (in dark) and 2.360 and 267 Ω (under 200 W), respectively. Cheung's and Norde functions were also used and the obtained R_s values from each method are stated out to be consistent, having decreasing trends with increasing illumination. These experimental results are a strong evidence of the fabricated Au/ZnO/n-GaAs SBDs exhibits a photodiode behavior. The increase in n with illumination can be explained by assuming inhomogeneities of BH and N_{ss} at M/S interface, interfacial ZnO layer, generation-recombination within the space charge region and R_s. The energy distribution profiles of surface states (N_{ss}) were acquired from the forward biases I–V data by considering voltage dependent Φ_e and n and R_s. The N_{ss} vs ($E_c - E_{ss}$) plots have U shape behavior and increase with the increment of the illumination levels. The N_{ss} values found in view of R_s values are lower than those found by ignoring the R_s especially near conductance band. As a result, surface states which are in-equilibrium with semiconductor can serve as recombination centers and have a crucial mission especially in reverse bias I–V characteristics.

References

1. E.H. Rhoderick, *Metal-Semiconductor Contacts* (Oxford University Press, Oxford, 1978)
2. K. Kano, *Semiconductor Devices* (Prentice-Hall, Upper Saddle River, 1998)
3. A. Kaya, E. Marıl, Ş. Altındal, İ. Uslu, Microelectron. Eng. **185**, 166–171 (2016)
4. E. Marıl, A. Kaya, S. Koçyiğit, Ş. Altındal, Mater. Sci. Semicond. Proc. **31**, 256–261 (2015)
5. B.L. Sharma, *Metal-Semiconductor Schottky Barrier Junctions and Their Applications* (Plenum Press, New York, 1984)
6. N. Başman, O. Uzun, S. Fiat, C. Alkan, G. Çankaya, J. Mater. Sci. Mater. Electron. **13**, 273–275 (2002). doi:10.1007/s10854-012-0819-1
7. S. Demirezen, Ş. Altındal, İ. Uslu, Current Appl. Phys. **13**, 53–59 (2013)
8. P. Macháč, V. Peřina, J. Mater. Sci. Mater. Electron. **23**, 2282–2288 (2012)
9. S.M. Sze, *Physics Semiconductor Devices* (Wiley, New York, 1981), pp. 24–30
10. M. Mamor, K. Bouziane, A. Tirbiyine, H. Alhamrashdi, Superlattices Microstruct. **72**, 344–351 (2014). doi:10.1016/j.spmi.2014.05.012
11. T.S. Huang, R.S. Fang, Solid State Electron. **37**, 1652–1661 (1994). doi:10.1016/0038-1101(94)90152
12. M. Soylu, F. Yakuphanoglu, Superlattices Microstruct. **52**, 470–483 (2012). doi:10.1016/j.spmi.2012.05.022
13. A.F. Özdemir, A. Türüt, A. Kökce, Thin Solid Films **425**, 210–215 (2003)
14. M.E. Aydın, M. Soylu, F. Yakuphanoglu, W.A. Farooq, Microelectron. Eng. **88**, 867–871 (2011). doi:10.1016/j.mee.2010.11.012
15. S. Demirezen, E. Özavcı, Ş. Altındal, Mater. Sci. Semicond. Proc. **23**, 1–6 (2014). doi:10.1016/j.mssp.2014.02.022
16. J.M. Borrego, R.J. Gutmann, S. Ashok, Solid State Electron. **20**, 125–132 (1977)
17. F.A. Padovani, G.G. Sumner, J. Appl. Phys. **36**, 3744–3747 (1965)
18. V.R. Reddy, V. Janardhanam, M.-S. Kang, C.-J. Choi, J. Mater. Sci. Mater. Electron. **25**, 2379–2386 (2014). doi:10.1007/s10854-012-0819-1
19. E. Özavcı, S. Demirezen, U. Aydemir, Ş. Altındal, Sens. Actuators A **194**, 259–268 (2013). doi:10.1016/j.sna.2013.02.018
20. Ö. Güllü, M. Biber, S. Duman, A. Türüt, Appl. Surf. Sci. **253**, 7246–7253 (2007). doi:10.1016/j.apsusc.2007.03.002
21. M.K. Hudait, P. Venkateswarlu, S.B. Krupanidhi, Solid State Electron. **45**, 133–141 (2001)
22. T.T.A. Tuan, D.-H. Kuo, C.-C. Li, W.-C. Yen, J. Mater. Sci. Mater. Electron. **25**, 3264–3270 (2014). doi:10.1007/s10854-014-2012-1
23. İ. Yücedağ, A. Kaya, H. Tecimer, Ş. Altındal, Mater. Sci. Semicond. Proc. **28**, 37–42 (2014). doi:10.1016/j.mssp.2014.03.051
24. H. Tecimer, A. Türüt, H. Uslu, Ş. Altındal, İ. Uslu, Sens. Actuators A **199**, 194–201 (2013). doi:10.1016/j.sna.2013.05.027
25. J. Werner, H. Guttler, J. Appl. Phys. **69**, 1522–1533 (1991)
26. G.B. Sakr, I.S. Yahia, J. Alloys Compd. **503**, 213 (2010)

27. J.K. Jha, R.S. Ortiz, J. Du, N.D. Shepherd, J. Mater. Sci. Mater. Electron. **25**, 1492–1498 (2014). doi:10.1007/s10854-014-1758-9
28. C. Tsiarapas, D. Girginoudi, N. Georgoulas, Superlattices Microstruct. **75**, 171–182 (2014). doi:10.1016/j.spmi.2014.07.041
29. C.S. Singh, G. Agarwal, G. DurgaRao, S. Chaudhary, R. Singh, Mater. Sci. Semicond. Proc. **14**, 1–4 (2011). doi:10.1016/j.mssp.2010.12.009
30. B.K. Singh, S. Tripathi, Superlattices Microstruct. **85**, 697–706 (2015). doi:10.1016/j.spmi.2015.06.038
31. A. Sarıyıldız, Ö. Vural, M. Evecen, Ş. Altındal, J. Mater. Sci. Mater. Electron. **25**, 4391–4397 (2014). doi:10.1007/s10854-014-2178-6
32. M.O. Aboelfotoh, J. Appl. Phys. **69**, 3351 (1991)
33. A. Tataroğlu, Ş. Altındal, Microelectron. Eng. **85**, 233–237 (2008). doi:10.1016/j.mee.2007.05.043
34. H.C. Card, E.H. Rhoderick, J Phys D **4**, 1589 (1971)
35. J.H. Werner, Appl. Phys. A **47**, 291 (1988)
36. Ş. Altındal, S. Karadeniz, N. Tuğluoğlu, A. Tataroğlu, Solid State Electron. **47**, 1847–1854 (2003)
37. P. Chattopadhyay, Solid State Electron. **37**, 1759 (1994). doi:10.1016/0038-1101(94)90223-2
38. H. Uslu, Ş. Altındal, U. Aydemir, İ. Dokme, İ.M. Afandiyeva, J. Alloy. Compd. **503**, 96–102 (2010). doi:10.1016/j.jallcom.2010.04.210
39. A. Kaya, Ö. Vural, H. Tecimer, S. Demirezen, Ş. Altındal, Current Appl. Phys. **14**, 322–330 (2014). doi:10.1016/j.cap.2013.12.005
40. S.K. Cheung, N.W. Cheung, Appl. Phys. Lett. **49**, 85 (1986)
41. Amir Hussain, Atowar Rahman, Superlattices Microstruct. **80**, 39–52 (2015). doi:10.1016/j.spmi.2014.12.030
42. A.A.M. Farag, I.S. Yahia, M. Fadel, Int. J. Hydrogen Energy **34**, 4906 (2009). doi:10.1016/j.ijhydene.2009.03.034
43. S.A. Yerişkin, H. Uslu, T. Tunç, Ş. Altındal, Int. Congr. Adv. Appl. Phys.Mater. Sci. AIP Conf. Proc. **1400**, 541–545 (2011). doi:10.1063/1.3663178
44. F. Yakuphanoğlu, K. Mensah-Darkwa, A.A. Al-Ghamdi, R.K. Gupta, W.A. Farooq, Microelectron. Eng. **154**, 53–61 (2016). doi:10.1016/j.mee.2016.03.001
45. M.Y. Feteha, M. Soliman, N.G. Gomaa, M. Ashry, Renew. Energy **26**, 113 (2002). doi:10.1016/S0960-1481(01)00102-1